

Supplementary Material for Multi-Contrast MRI Conditioned, Adaptive Adversarial Diffusion Model for High-Fidelity MRI Synthesis

Sanuwani Dayarathna¹ Kh Tohidul Islam² Bohan Zhuang¹ Guang Yang³ Jianfei Cai¹
Meng Law¹ Zhaolin Chen^{1,2}

¹ Monash University, Australia ²Monash Biomedical Imaging, Australia ³Imperial College, United Kingdom

1. More Analysis of Results

1.1. Evaluation Metrics

To evaluate the performance of the proposed approach, we employ structural similarity index (SSIM) and peak signal-to-noise ratio (PSNR) metrics. PSNR measures the quality of the synthesized images which is defined as,

$$PSNR = 10 \cdot \log_{10} \left(\frac{MAX_I^2}{MSE(\bar{Y}(x), Y(x))} \right) \quad (1)$$

where Y and \bar{Y} is real and x images and represents aligned pixels. MAX_I^2 gives the maximum intensity value of the images and MSE represents the Mean Squared Error between Y and \bar{Y} . SSIM assesses the structural similarity between the synthesized and real images as follows.

$$SSIM(\bar{Y}, Y) = \frac{(2\mu_{\bar{Y}}\mu_Y + C_1)(2\sigma_{\bar{Y}Y} + C_2)}{(\mu_{\bar{Y}}^2 + \mu_Y^2 + C_1)(\sigma_{\bar{Y}}^2 + \sigma_Y^2 + C_2)} \quad (2)$$

where μ_Y , $\mu_{\bar{Y}}$ represents the mean values of Y and \bar{Y} , while σ_Y , $\sigma_{\bar{Y}}$ represents the covariance of Y and \bar{Y} . C_1 and C_2 are two variables that are used to stabilize the division by avoiding the null denominator. Prior to calculating these metrics, we normalized our images using their maximum intensity and applied the same evaluation criteria to all comparison methods to ensure a fair comparison.

1.2. Distribution of Structural Similarity

To evaluate the distribution of structural similarity, we plotted box plots of SSIM values across the test dataset for McCaD and other comparison methods as in Fig. 1. The horizontal bar within the boxplot represents the median SSIM value, while the whiskers indicate the minimum and maximum values, with scatter points showing outliers. The plots for different synthesis tasks clearly demonstrate higher median values for McCaD compared to all baselines. Additionally, the smaller interquartile range compared to other distributions indicates better performance, suggesting that

McCaD’s synthesis performance is more robust and consistently produces high-quality results across different synthesis tasks with fewer outliers. However, based on the presented results, it is clearly visible that although McCaD produces more robust results compared to other methods, it generates more outliers in tumor synthesis compared to healthy synthesis task. This can be mainly due to the intricate nature of the task, which involves the more complex synthesis of pathological information, which requires further analysis to understand and address these challenges.

1.3. Effect of Feature Components

To further evaluate the impact of the feature components (FM and FA loss), we provided a visual comparison of the synthesis results with and without these components in Fig. 2. These components primarily focus on improving the perceptual quality of the synthetic results for high-fidelity sample generation. The corresponding error maps indicate that although the synthesis results visually appear more similar to the ground truths without the feature components, they exhibit significant errors compared to the synthesis results with the feature components, particularly in capturing more precise boundary information in tumor regions.

1.4. Effect of Multi-contrast MRI Synthesis

We also demonstrated the enhancement in performance achieved through multi-contrast imaging with a visual comparison of the synthetic results between the multi-contrast and single-contrast scenarios in Fig. 3. The visualization of the results clearly shows the enhancement in the synthesis of tumor regions by incorporating another MRI contrast, leading to a more precise and accurate synthesis. T1w predominantly contributes to preserving the underlying anatomical structural details in the synthesized FLAIR image. However, it lacks the intricate pathological features found in the tumor region, which are primarily derived from the T2w image. As a result, the accuracy in representing the tumor region is reduced.

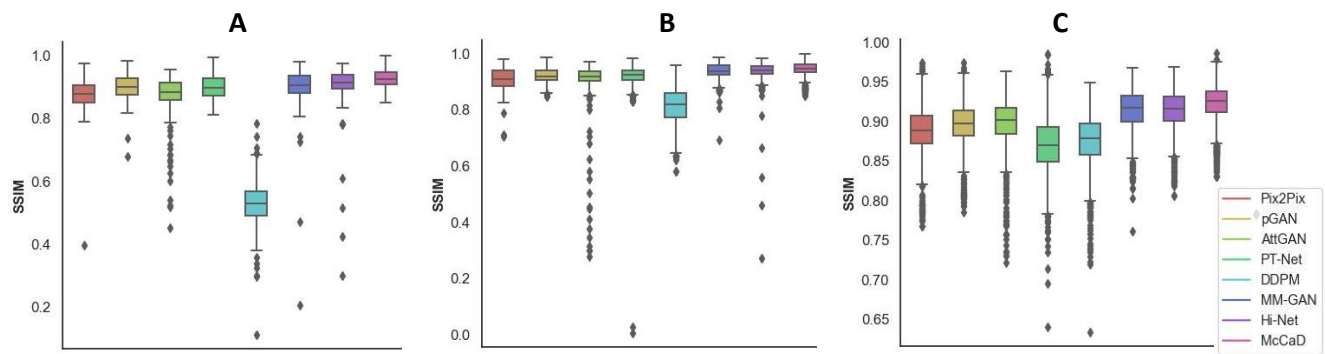


Figure 1. Distribution of SSIM values across different synthesis methods for (A). T2w, (B) FLAIR synthesis from the healthy dataset and (C) T2w synthesis from the tumor dataset.

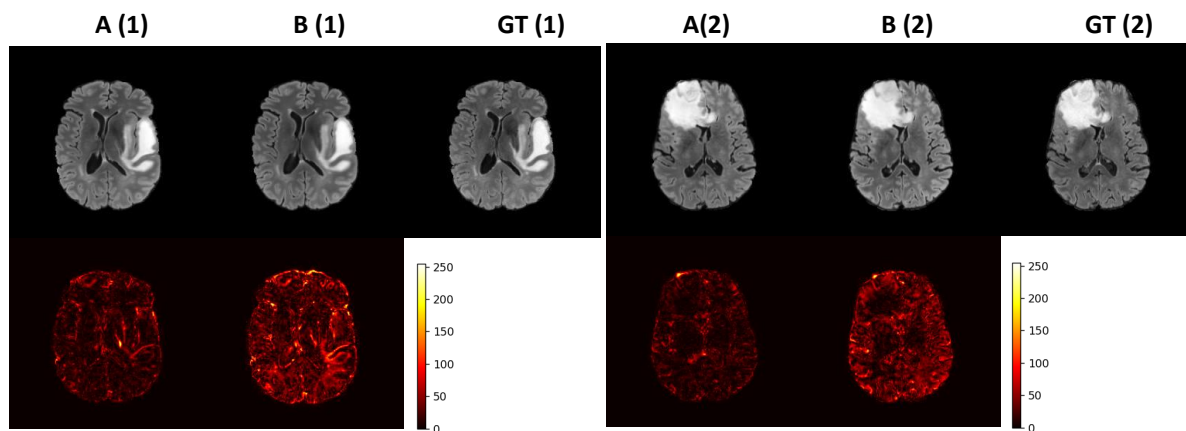


Figure 2. Visualization of FLAIR synthesis from BraTS dataset with and w/o feature components. A (1) and A(2) show the synthesized results with feature components, and B(1) and B(2) show the synthesis results w/o feature components. GT(1) and GT(2) show the corresponding ground truth images of the two synthesized scenarios 1 and 2. The second row shows error maps for each synthesized contrast.

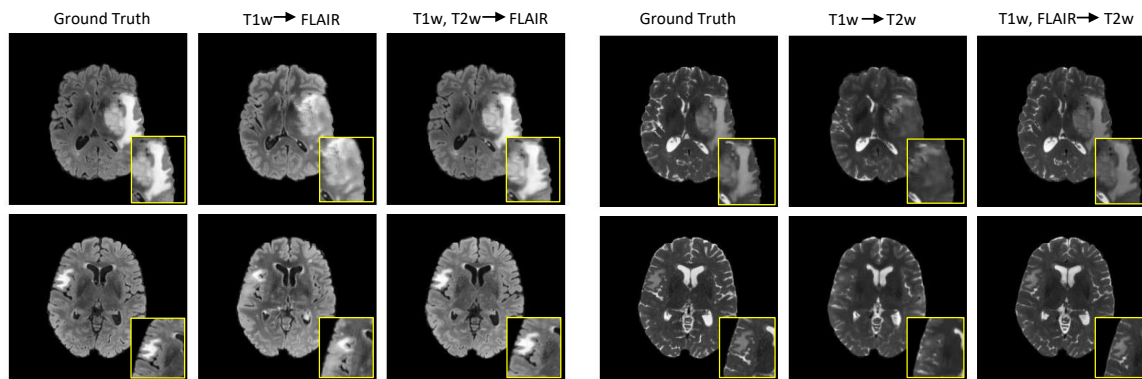


Figure 3. Visualization of T2w and FLAIR synthesis from BraTS dataset for single image conditioning and multi-contrast conditioning.